Hindawi
Advances in Polymer Technology
Volume 2021, Article ID 5175473, 10 pages
https://doi.org/10.1155/2021/5175473

Research Article

Supramolecular Assembly and Reversible Transition and of Chitosan Fluorescent Micelles by Noncovalent Modulation

An Liu,[1] Hong Song,[1] Puyou Jia,[2] Ying Lin,[1,2] Qingping Song,[1] and Jiangang Gao[1]

[1]*Anhui Laboratory of Clean Catalytic Engineering, School of Chemical and Environmental Engineering, Anhui Polytechnic University, Wuhu 241000, China*
[2]*Jiangsu Key Laboratory for Biomass Energy and Material, Institute of Chemical Industry of Forest Products, Chinese Academy of Forestry (CAF), Nanjing 210042, China*

Correspondence should be addressed to Puyou Jia; jiapuyou@icifp.cn, Ying Lin; liny@ahpu.edu.cn, and Jiangang Gao; gaojiangang@ahpu.edu.cn

Received 13 July 2021; Revised 9 October 2021; Accepted 18 October 2021; Published 12 November 2021

Academic Editor: Alain Durand

Chitosan-based intelligent artificial systems have been of increasing interest for their biocompatibility, multifunctionality, biological activity, and low cost. Herein, we report the fabrication of supramolecular nanoparticles based on water-soluble chitosan (WCS) and 1,1′,1″,1‴-(ethene-1,1,2,2-tetrayl)tetrakis(benzene-4,1-diyl) tetrakis(azanediyl)tetraacetic acid (TPE-(N-COOH)$_4$), which is capable of reversible transition between polyion complexes (PICs) and hydrogen bonding complexes (HBCs) with tunable aggregation-induced emission driven by pH value. The PIC micelles could be formed via electrostatic interaction between ammonium cations and carboxylate anions under mild alkaline conditions. The formation of the micelles dramatically blocks the nonradiative pathway and enhances the fluorescence of TPE moieties, and the maximum fluorescence intensity was achieved near the isoelectric point due to the restriction of intramolecular motion. In addition, the fluorescence intensity and size of the PIC micelles exhibited a temperature response in the range from 20 to 80°C. Upon adjusting the solution pH to 2, the PIC micelles were reconstructed into hydrogen-bonding complexes while the hydrogen bonding interaction between the protonated carboxyl groups of TPE-(N-COOH)$_4$ and chitosan. Moreover, the size of the micelles underwent a remarkable decrease, whereas the fluorescence emission was further enhanced by ~6.25-fold. The pH actuated micellar transition from PIC to HBC with tunable fluorescence performance is fully reversible. This study provides novel multifunctional materials that are of great importance for their potential application in the fields of optoelectronic devices and chemical and biomedical sensors.

1. Introduction

Recently, stimulation responsive functionalized polymeric micelles have drawn considerable attention because they have distinctive photophysical properties and potential applications in life sciences [1–3]. Among them, the utilization of noncovalent interactions to self-assemble nature macromolecules with the formation of hierarchical assemblies is of enormous importance. In fact, the biomimicking of noncovalent interactions and their microenvironment triggered transitions in biological systems to fabricate biomedical materials has been a subject of considerable interest [4, 5]. Accordingly, a great variety of supramolecular interactions have been developed and investigated to construct numerous functional architectures, including host-guest interaction, coordination interaction, electrostatic interaction, hydrophobic association, π-π stacking, and hydrogen bonding [6–10]. For example, the electrostatic interaction has performed an extensive effect on the controlled drug delivery and interprotein recognition [11, 12], whereas hydrogen bonding interaction has dominated shape self-recovery and volume regulation of the vesicles constructed from polysaccharide and embodying cell like behavior [13]. The polyion complex (PIC) was constructed through electrostatic interaction originally proposed by Kataoka [14, 15], while inter/intramolecular hydrogen bonding promoted the formation of hydrogen bonding complexes

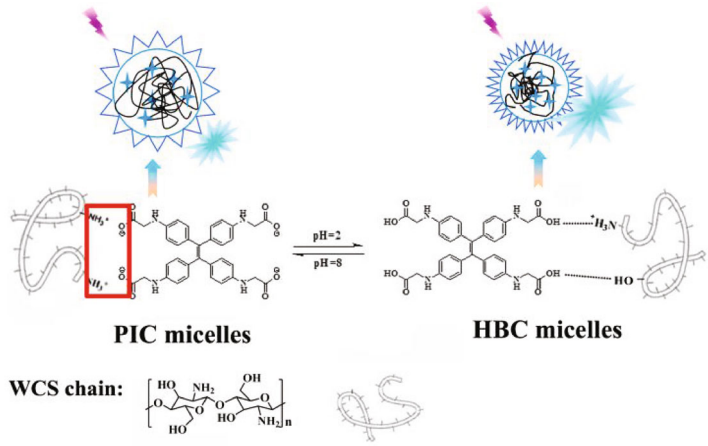

Scheme 1: Schematic illustration of self-assembly between TPE-(N-COOH)$_4$ and chitosan via different interactions to form PIC and HBC micelles, respectively, under acid-based-controlled condition. The pH-mediated transformation of PIC to HBC micelles marked by AIE enhancement is reversible.

(HBCs). Thus, the advance of noncovalent interactions will not only enrich the family of biomimetic nanostructures, but also provide a new bridge between the colloidal and life sciences [7, 16–19].

Generally, the amphiphilic copolymers could self-assemble to form well-defined nanostructures with reversed and stimuli-responsive features. Taking advantage of dynamic nature of noncovalent interactions, a diversity of synthetic systems were developed for schizophrenic self-assembly behavior [20–23]. Stuart and co-workers used diblock copolymers, oligoligands, and metal ions to devise inverted nanoparticles with excellent salt stability and magnetic relaxation properties [24, 25]. However, the syntheses of amphiphilic macromolecules by traditional covalent chemistry are typically time consuming and cost intensive. Along this line, the widespread attention has been paid to nature polymers with abundant functional groups. Especially, chitosan is considered as outstanding candidates, since it is rich groups, good biocompatibility, biodegradability, and wide source. To date, chitosan has been employed to assemble with functional molecules through the noncovalent interaction in solution resulting in supramolecular structures with various morphologies because of the convertibility between amino and ammonium salts [26, 27]. Numerous chitosan-based supramolecular assemblies with special architectures and functions have been synthesized and investigated for applications in versatile fields, such as drug delivery, bioimaging, biosensing, antibacterial, wastewater treatment, and packing [28–30]. Given the crucial roles of noncovalent interactions in biological systems, we hypothesized that it was highly beneficial to construct new schizophrenic systems on the basis of the chitosan, which may be favorable for developing novel biomimetic materials.

The traditional organic fluorescent materials show significantly light-emitting behaviors in dilute solutions but weak emission in concentrated solutions, which is generally considered a thorny obstacle to the practical applications. The concept of aggregation-induced emission (AIE) [31] or aggregation-induced emission enhancement (AIEE) [32] has emerged to be a powerful strategy for the design of novel types of fluorescent devices [33, 34]. In order to have an in-depth understanding of working mechanism, typical AIE-active molecules such as tetraphenylethene (TPE) have been employed to develop assemblies of various structures [35]. Obviously, aggregates formed by the noncovalent interactions between the multivalent polyelectrolytes and AIE molecules can provide an effective way toward the formation of reversible configuration and luminescent system. Therefore, it is expected that the applications of these "smart" assemblies have been expanded into many fields, such as bioprobes, fluorescence sensors, bioimaging, and organic light-emitting diodes [21, 24, 36].

In the present work, we report the fabrication of a novel supramolecular system comprising two functional components, namely chitosan and TPE derivative bearing four carboxyl acid moieties (TPE-(N-COOH)$_4$), that can form two distinct micelles with fully inverted structures in response to pH changes (Scheme 1). The chitosan provides biological activity to micelles, while TPE-(N-COOH)$_4$ endows them controllable fluorescence properties. Under mild alkaline conditions, the electrostatic association between the chitosan bearing amino cations and the carboxylate anions of TPE-(N-COOH)$_4$ can generate PIC micelles. Significantly, along with the PIC micelle formation, the fluorescence emission of TPE moieties was gradually "turn on" because of the restriction of intramolecular motion. Alternatively, after lowering the solution pH to 2, the protonated carboxyl groups of tetracarboxylated TPE serving as hydrogen bonding donor or acceptors can interact with the hydroxyl or amino groups in the chitosan to constitute the HBC micelles. Furthermore, the pH-mediated conformational transition of micelles enhanced the fluorescence emission of the system, presumably due to the deep fixation of the TPE chromophore within HBC micelles. Especially, the pH-dependent transition with reversed micellar structures and tunable fluorescence performance is fully reversible, as shown in Scheme 1.

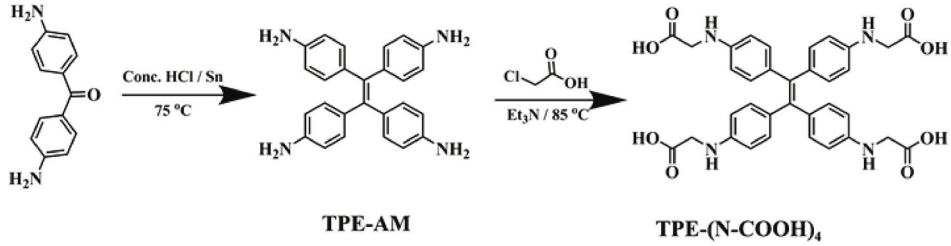

Scheme 2: Synthetic routes employed for the preparation of TPE-(N-COOH)$_4$.

2. Materials and Methods

2.1. Materials. Water-soluble chitosan (WCS, 85~90% deacetylated) with number-average molecular weight (Mn) of 5 kDa was purchased from Yuhuan Biomedical Company (Zhejiang, China). 4,4′-Diaminobenzophenone and Tin were obtained from Adamas Reagent, Ltd. (Shanghai, China). Chloroacetic acid and triethylamine (TEA) were supplied by Sinopharm Chemical Reagent Co. Ltd. (Shanghai, China). All other reagents were of analytical grade and used without further purification. Distilled water was used throughout all experiments.

2.2. Synthesis of 1,1′,1″,1‴-(Ethene-1,1,2,2-Tetrayl) Tetrakis(Benzene-4,1-Diyl) Tetrakis(Azanediyl)Tetraacetic Acid (TPE-(N-COOH)$_4$). Synthesis schemes employed for the preparation of TPE-(N-COOH)$_4$ are shown in Scheme 2. 4,4′,4″,4‴-(ethene-1,1,2,2-tetrayl)tetraaniline (TPE-AM) was synthesized at first following the procedures reported previously with minor modifications [37]. Briefly, 0.8 g of 4,4′-diaminobenzophenone was dissolved in 35 mL concentrated hydrochloric acid under heating and stirring. Then, 3.0 g of Tin powder was added, and the reaction mixture was stirred at 75°C for 6 h. After cooling, the mixture was filtered and washed with NaOH (1 M) and water. The product was obtained as a yellowish powder (685 mg, yield ~85%) after dried under vacuum.

TPE-AM was then reacted with chloroacetic acid to afford the target product, TPE-(N-COOH)$_4$. In a typical procedure, 1.0 g of TPE-AM and 2.0 g chloroacetic acid were dissolved in 15 mL toluene under stirring, and triethylamine (3 mL) was then added. The mixture was heated to 85°C and kept stirring for 6 h. Thereafter, the resulting mixture was cooled to room temperature and washed with saturated $NaHCO_3$ aqueous solution. The product was collected by filtration, washed twice with ether, and dried to afford a yellowish power (830 mg) in 53% yield. The structure of TPE-AM and TPE-(N-COOH)$_4$ was confirmed by ^{1}H NMR and FT-IR spectra.

2.3. Preparation of PIC Micelles. The micelles were prepared by mixing negatively charged TPE-(N-COOH)$_4$ and positively charged WCS with dropping method. Firstly, stock solution of TPE-(N-COOH)$_4$ with a concentration of 1.0 g/L and pH = 8 was prepared. Then, WCS aqueous solution was added dropwise into equal volume of the stock solution of TPE-(N-COOH)$_4$ under stirring, and opalescent suspension was formed. The concentrations of all WCS solution were adjusted according to requirements of optical tracer.

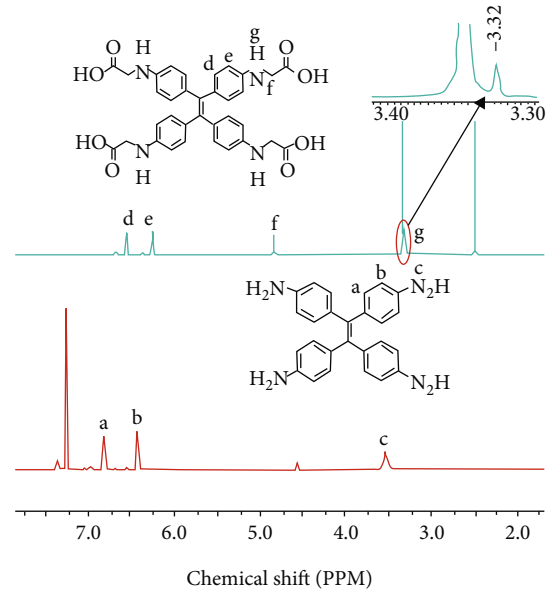

Figure 1: ^{1}H NMR spectrum of TPE-(N-COOH)$_4$ in d_6-DMSO (up) and TPE-AM in $CDCl_3$ (bottom).

2.4. Characterization. All ^{1}H NMR spectra were recorded on a Bruker AVANCE III HD spectrometer with tetramethylsilane as internal standard. Fourier transform infrared (FT-IR) spectra were performed on a Nicolet 510p spectrometer. Morphology of the micelles was observed using transmission electron microscopy (TEM) (HT-7700, Hitachi) and scanning electron microscopy (SEM) (S-4800, Hitachi). A Brookhaven BI9000 AT system (Brookhaven Instruments Co., USA) was employed for dynamic light scattering (DLS) measurements, and the hydrodynamic diameter and distribution of micelles were computed. The zeta potential of the micelles was obtained with a Zetaplus (Brookhaven Instruments Corporation). All results were the average of triplicate measurements. The photoluminescence (PL) spectra were collected using an RF-5301PC spectrofluorometer (Shimadzu). The slit widths were set at 5 nm for both excitation and emission.

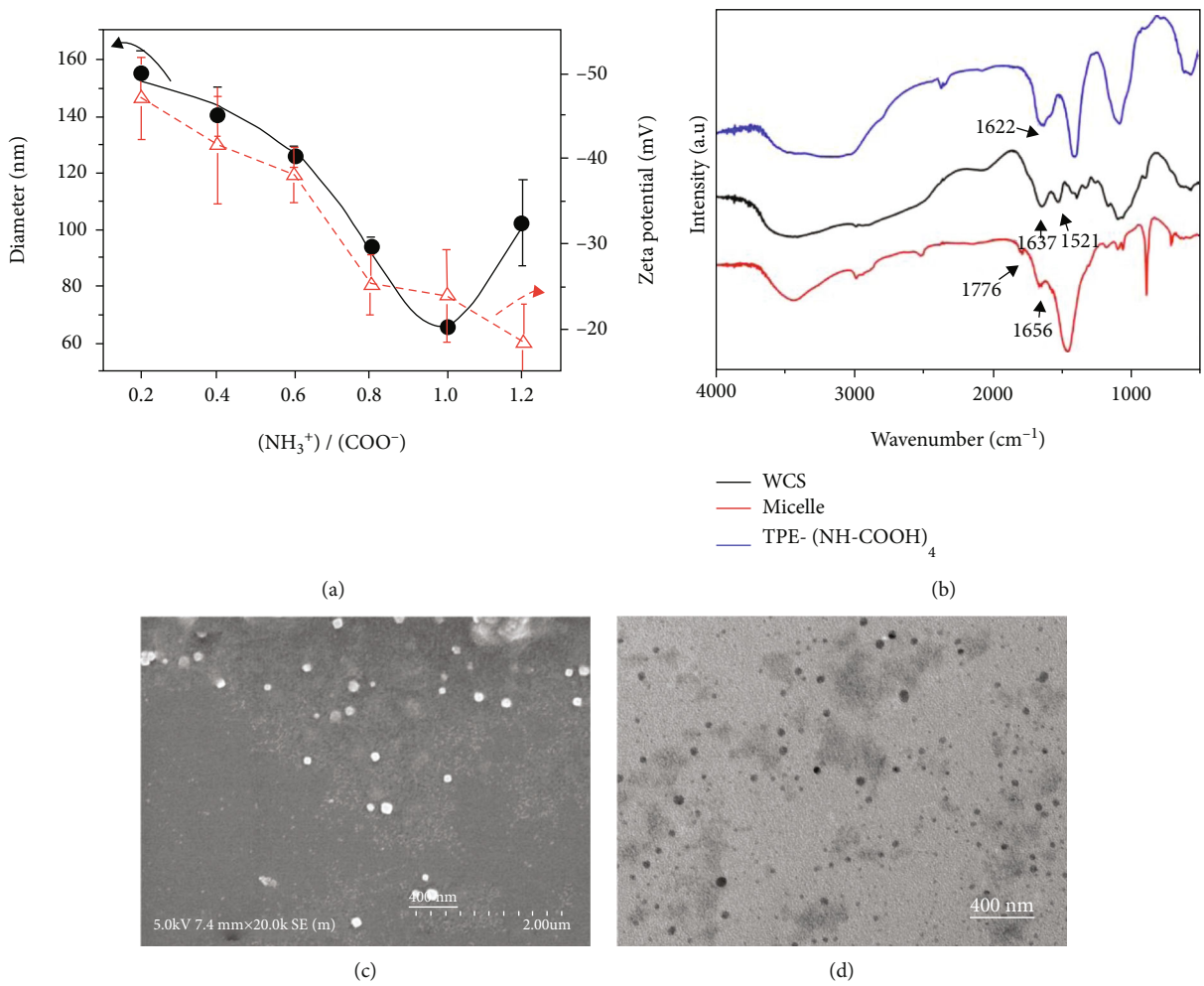

FIGURE 2: (a) The average hydrodynamic diameters and zeta potential of micelles as a function of $[NH_3^+]/[COO^-]$ ratio upon mixing WCS and TPE-$(N\text{-}COOH)_4$ at pH = 8. (b) FT-IR spectra of WCS, TPE-$(N\text{-}COOH)_4$, and PIC micelles. (c) Typical SEM and (d) TEM images of the micelles with charge ratio (+/-) of 1.0.

3. Results and Discussion

3.1. Preparation and Characterization of PIC Micelles. As one of the typical AIE-active molecules, TPE derivatives have been widely used in sensing field with analytes ranging from thiols, gas, heavy-metal ions to biomacromolecules [22, 38]. Here, to build fluorescent micelles based on the electrostatic interaction, tetracarboxylated TPE derivative (TPE-$(N\text{-}COOH)_4$) was synthesized at first via two steps according to Scheme 2. The ^{1}H NMR spectra of the synthesized TPE derivatives are shown in Figure 1. As marked in Figure 1, the characteristic signals from TPE-AM (δH^a 6.82 ppm, 8H Ar**H**; δH^b 6.43 ppm, 8H Ar**H**; and δH^c 3.54 ppm, 8H -N**H**$_2$) and TPE-$(N\text{-}COOH)_4$ (δH^d 6.57 ppm, 8H Ar**H**; δH^e 6.26 ppm, 8H ArH; δH^f 4.84 ppm, 8H -C**H**$_2$COO-; and δH^g 3.32 ppm, 4H -N**H**CH$_2$-) can be clearly observed, indicating the successful synthesis of the compounds. The three peaks of TPE-AM at 6.82 ppm, 6.43 ppm, and 3.54 ppm were assigned to the protons of the phenyl ring (a and b) and amino group (c), respectively. By comparison, the ^{1}H NMR spectrum of TPE-$(N\text{-}COOH)_4$ shows a new peak at 4.84 ppm, corresponding to the protons on the methylene (f) of the acetyl group.

Being a cationic biopolymer bearing amino group, chitosan chains undergo counterion complexation in aqueous solution with many multivalent anionic substances, such as EDTA and poly(acrylic acid) [26, 27], to fabricate colloidal aggregates. Here, the inter- and intramolecular linages occurred between carboxyl groups from TPE-$(N\text{-}COOH)_4$ and positively charged amino groups of WCS, resulting in the formation of micelles with hydrophilic WCS coronas. Figure 2(a) depicts the change of average hydrodynamic diameter and zeta potential of micelles introducing cationic WCS into the aqueous solution of TPE-$(N\text{-}COOH)_4$ at pH = 8. It can be found that the diameter underwent a gradual decrease prior to the arrival of the isoelectric point ($[NH_3^+]/[COO^-] = 1.0$), whereas it exhibited a significant increase from 65 nm to 102 nm when the charge ratio of $[NH_3^+]/[COO^-]$ increased from 1.0 to 1.2. The polydispersity index of every case was approximately 0.3, indicative

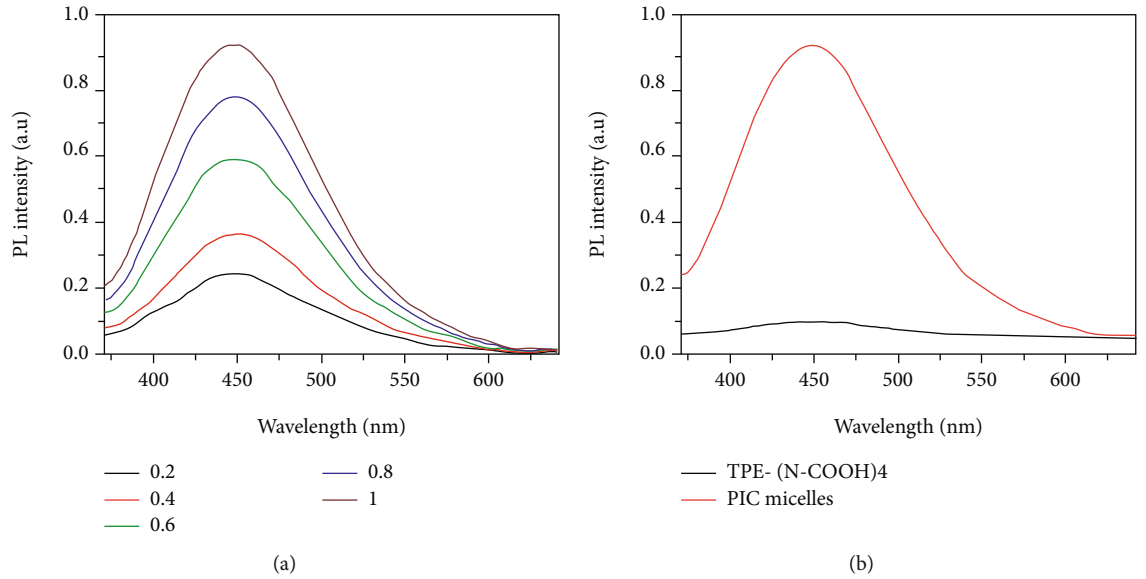

Figure 3: (a) Fluorescence spectra of PIC micelles formed from WCS and TPE-(N-COOH)$_4$ in aqueous solution with different ratio of [NH_3^+]/[COO^-]. (b) Fluorescence spectra obtained for TPE-(N-COOH)$_4$ aqueous solution and PIC micelles assembled from WCS and TPE-(N-COOH)$_4$ at the [NH_3^+]/[COO^-] molar ratio of 1.0. pH = 8, λ_{ex} = 345 nm. The TPE-(N-COOH)$_4$ concentration was fixed at 1.0 g/L in all case. The emission intensities measured at various ratios were normalized to the initial intensity.

of a broader size distribution. Also, the zeta potential of the micelles shows a negative value in the range of feed ratio observed. The micelle structure was also confirmed by FT-IR analysis, as shown in Figure 2(b). For PIC micelles, the intensities of amide band II at 1521 cm^{-1} and amide I at 1637 cm^{-1}, which can be observed clearly in pure chitosan, decrease dramatically, and two new characteristic peaks appeared at 1776 cm^{-1} and 1656 cm^{-1}, which were assigned to the absorption of the carboxyl groups of TPE-(N-COOH)$_4$ (the absorption peak of carboxyl groups in pure tetracarboxylated TPE appears at 1622 cm^{-1}), and the NH_3^+ absorption of WCS, respectively, are observed. These changes in the FT-IR spectrum indicate that the carboxylic groups of TPE-(N-COOH)$_4$ are dissociated into COO^- groups which complex with protonated amino groups of WCS through electrostatic interaction to form the PIC micelles.

Particle morphology was then studied by electron microscopy. The SEM and TEM observations demonstrated that the obtained micelles were presented as spherical nanoparticles at the isoelectric point (Figures 2(c) and 2(d)). It is apparent that the nanoparticle size observed under SEM and TEM is smaller than the DLS result due to the shrinking in dry state. Hence, we can conclude that the most stable and compact PIC micelles can only be fabricated at the isoelectric point, which is consistent with the results of predecessors [20]. Additionally, due to the restriction of the intramolecular rotation of TPE-(N-COOH)$_4$ moieties within the PIC core, the self-assembling of micelles could be understood by the turn-on emission of TPE chromophores. Specific fluorescence titration spectroscopy with varying charge ratios revealed that the maximum emission intensity was achieved at the [NH_3^+]/[COO^-] molar ratio of 1.0, as shown in Figure 3. The result is in accordance with the trend of the hydrodynamic diameter variation of micelles. Therefore, we infer that the fluorescence intensity of the PIC micelles is strongly affected by the degree of electrostatic interaction between chitosan and tetracarboxylated TPE.

3.2. Response Behavior of Micelles. In view of the fabrication of PIC micelles, the research on the temperature response of micelles will be conducive to the development of their applications. Subsequently, the properties of self-assembled micelles against temperature variations were further conducted. Figure 4 shows the changes of the micelle size and light scattering intensity with temperature were monitored with the samples inside the DLS cuvette. On increasing the temperature of PIC micelle solution formed at the isoelectric point from 20 to 80°C, the scattered intensity underwent a pronounced drop though the hydrodynamic diameters kept almost constant over the same temperature range. This result indicates that the PIC micelles underwent gradual disintegration subjected to temperature rise. In other words, high temperature weakens the electrostatic interaction between opposite charges, leading to disintegration of micelles. As mentioned earlier, the electrostatic interaction between ammonium groups and carboxylate anions within micelles restrains the rotation of the phenyl groups of TPE-(N-COOH)$_4$ because of the spatial constraint, giving the enhanced fluorescence emission. Thus, it can be found that the fluorescence intensity of TPE moieties within the cores of PIC micelles gradually decreased subjected to temperature rise, as shown in Figure 4(c). On the other hand, high temperature weakens the restriction of rotation of the phenyl groups of TPE, resulting in a decrease of the fluorescence emission. Therefore, the PIC micelles incorporating TPE-(N-COOH)$_4$ fluorophores with unique temperature responsive characteristics could be employed as thermal sensors with tunable fluorescence emissions.

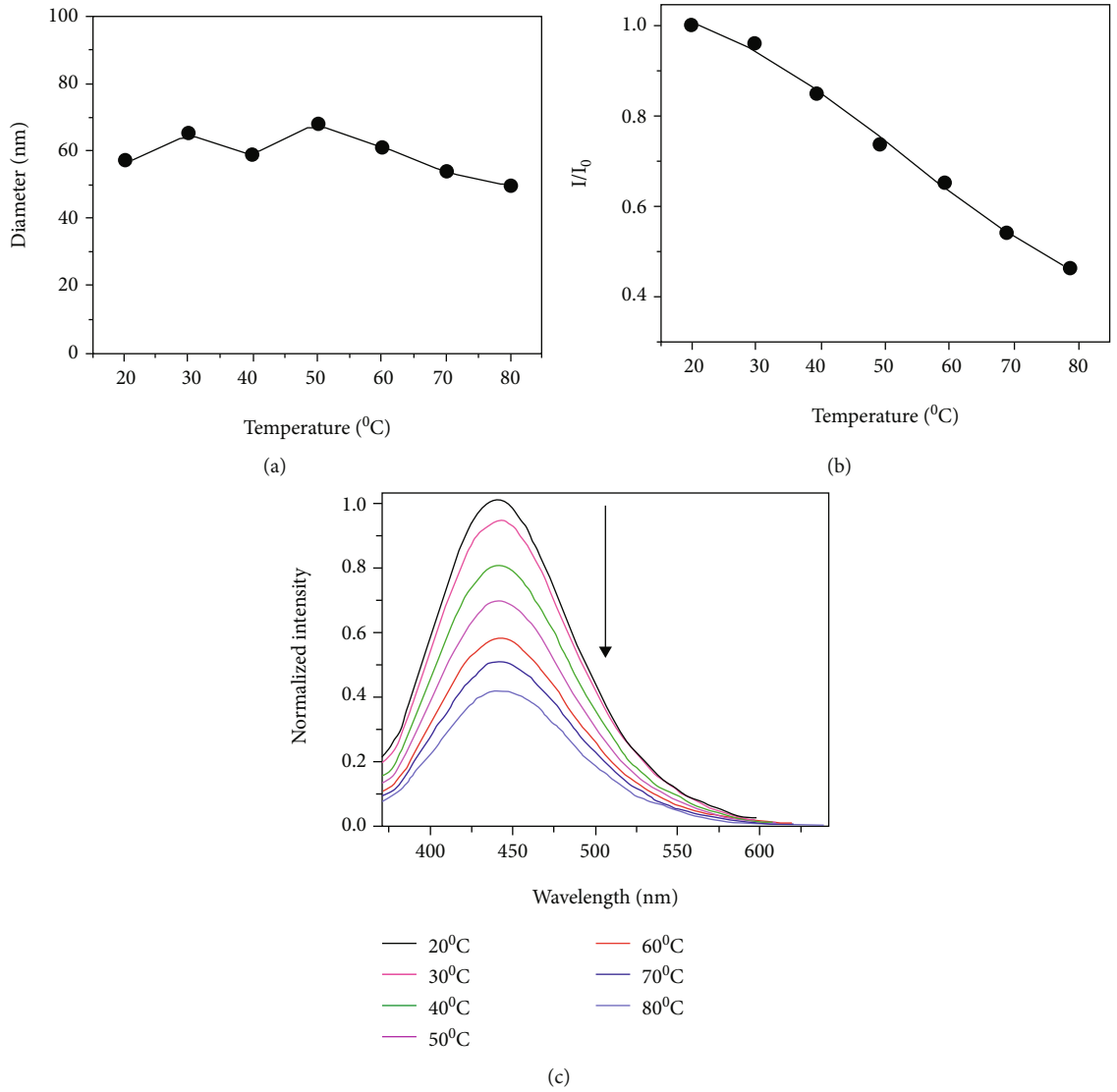

FIGURE 4: Temperature dependence of (a) average hydrodynamic diameters and (b) normalized scattering light intensity record for micelles composed by WCS and TPE-(N-COOH)$_4$ in aqueous solution at pH = 8. (c) Normalized fluorescence spectra of PIC micelles in aqueous solution versus temperature at pH = 8, λ_{ex} = 345 nm. The [NH_3^+]/[COO^-] molar ratio was 1.0.

As mentioned above, the increase in temperature can significantly weaken the stability of PIC micelles, leading to the disassembly of the WCS micelles and loss of TPE fluorescence. Based on similar considerations, it was postulated that the PIC micelles would probably disassemble with the decrease of solution pH as well, especially when the pH was lower than the pKa of carboxyl groups, due to protonation of carboxylate anions and thus eradication of electrostatic interaction between cationic chitosan and TPE-(N-COOH)$_4$. To further confirm the assumption, the performance of the micelles under acidic milieu was then evaluated. Under acidic condition, the TEM showed that the morphology of micelles became irregular but the particle size was significantly decreased (Figure 5(a)). Specifically, the hydrodynamic diameter of the micelles decreased from ~65 nm to ~26 nm upon pH drop from 8 to 2. Key determinants in the changes of particle size and intramicellar interaction were the ionization degrees of WCS and TPE-(N-COOH)$_4$ in different pH solution. The pKa values of carboxyl groups in TPE-(N-COOH)$_4$ and WCS are 2.6 and 6.5, respectively [26, 39]. At low pH, the carboxyl groups of tetracarboxylated TPE was almost protonated. It is noteworthy that the WCS with proton sponge effect can maintain complete or partial ionization in a wide pH range [40]. This result was confirmed by zeta potential measurements, as shown as in Figure 5(b). It can be seen that zeta potential of the micelles gradually increased from -23.9 mV to 42.2 mV with the decrease of pH from 8 to 2. The negative zeta potentials at a pH above 7.0 were mostly caused by the adsorption of anions, such as the OH^- [39]. Meanwhile, the fluorescence intensity of the micellar solutions exhibited a further 2.13-fold increase as compared to that of PIC micelles at pH = 8, as schematically shown in Figure 5(c). Correspondingly, the fluorescence band was blue shifted from 438 to 424 nm. The complexation of WCS/TPE-(N-COOH)$_4$ with protonated tetracarboxylated TPE not only

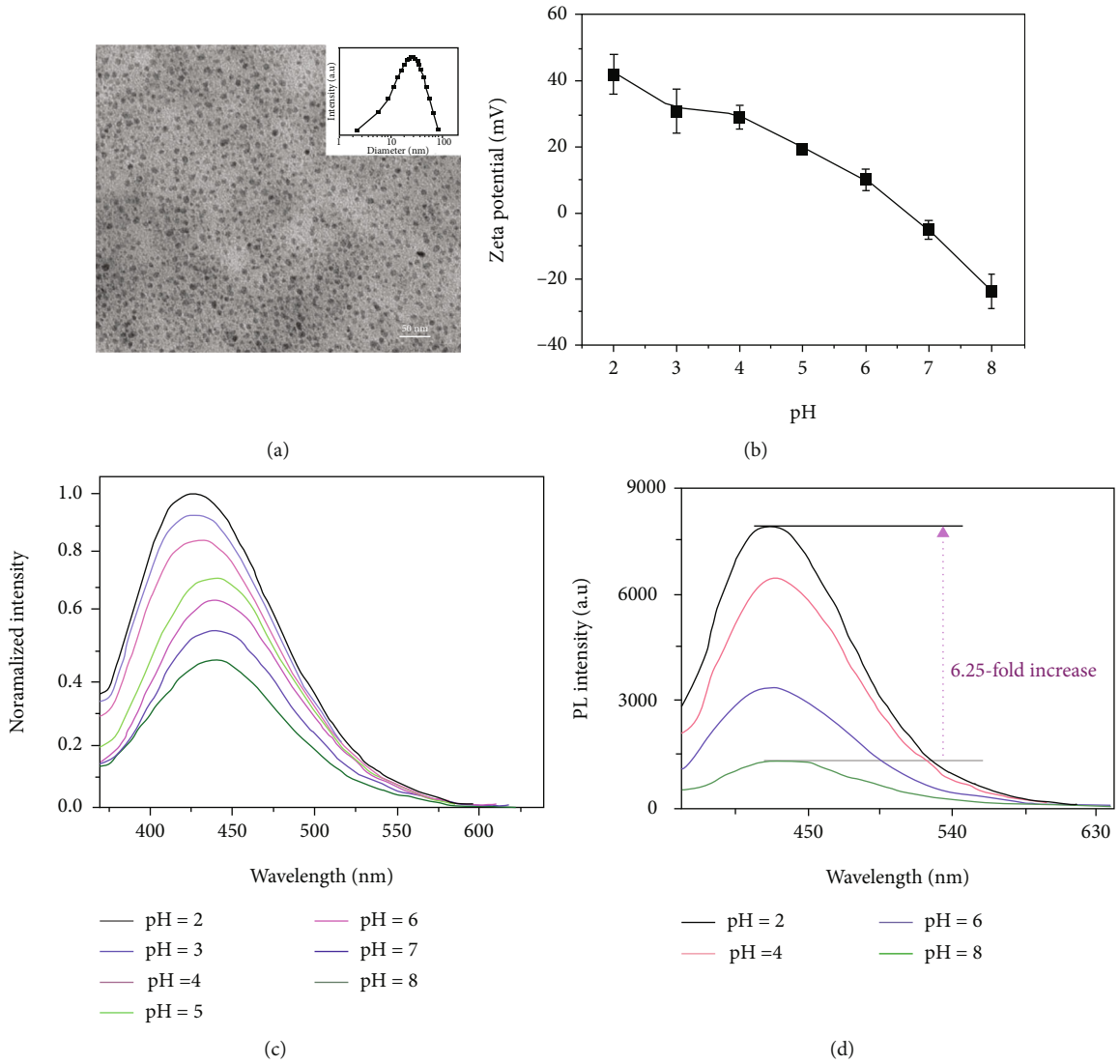

FIGURE 5: (a) TEM image of the micelles at pH = 2. Inset: size distributions of aqueous solutions of chitosan and TPE-(N-COOH)$_4$ mixture at pH = 2. (b) The zeta potential of micelles at different pH values. pH-dependence fluorescence emission spectra recorded for the aqueous solution of (c) WCS/TPE-(N-COOH)$_4$ micelles and (d) TPE-(N-COOH)$_4$ with pH decreasing from 8 to 2, λ_{ex} = 345 nm, 25°C. The molar ratio of [NH_3^+]/[COO^-] was 1.0, and the TPE-(N-COOH)$_4$ concentration was fixed at 1.0 g/L in all cases.

leads to a fluorescence enhancement feature but also a slight blue shift of 14 nm. The AIE enhancement feature accompanied by blue shifts occurred generally in systems containing small molecules with heteroatom-based groups [41].

To elucidate the underlying mechanism on aggregation-induced emission enhancement and the hydrodynamic diameter decrease subject to pH drop from 8 to 2, the fluorescence intensity changes of the pure TPE-(N-COOH)$_4$ solution under varying pH were detected as the control (Figure 5(d)). Upon decreasing pH from 8 to 2, the fluorescence intensity of TPE-(N-COOH)$_4$ fluorophores demonstrated a cumulative 6.25-fold increase, higher than that of the mixture of WCS/TPE-(N-COOH)$_4$ at the charge molar ratio (+/-) of 1.0 with the same TPE-(N-COOH)$_4$ concentration. Moreover, there was no shift of the emission band while the fluorescence was enhanced. It is concluded that there was a specific interaction between chitosan and protonated TPE-(N-COOH)$_4$ in acidic milieu, which prevented the hydrophobic TPE-(N-COOH)$_4$ molecules from precipitation. Considering the formation of much smaller assemblies at pH = 2, a possible common mechanism was introduced, the protonated TPE-(N-COOH)$_4$ served as the hydrogen bond donors or acceptors interacted with chitosan to form HBC micelles, on the surface of which positively charged WCS stabilized the hydrogen-bonded inner cores. Therefore, the hydrophobicity of AIE molecules and hydrogen bonding interaction within the HBC cores impeded the intramolecular rotation of TPE moieties and further boosted the fluorescence, because of the elimination of electrostatic repulsion of negatively charge TPE-(N-COOH)$_4$ under basic condition and the formation of more compact micelles with smaller size. Interestingly, the pH-mediated transitions in fluorescence intensity and hydrodynamic diameter were reversible with pH cycling between 8 and 2. The results

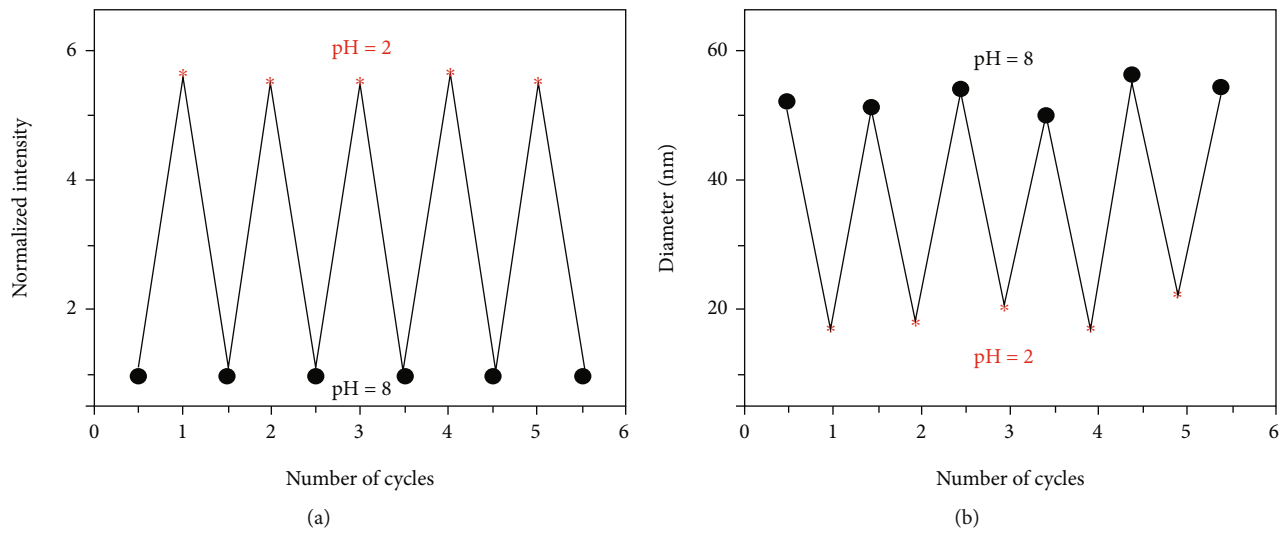

FIGURE 6: Evolutions of (a) normalized fluorescence intensity and (b) hydrodynamic diameters when pH was cycled between 2 and 8 (λ_{ex} = 345 nm, 25°C). The $[NH_3^+]/[COO^-]$ molar ratio was 1.0.

shown in Figure 6 illustrate that the TPE-$(N\text{-}COOH)_4$ moieties were fully protonated and hydrophobic at pH = 2, and the electrostatic interaction disappeared between the neutral TPE-$(N\text{-}COOH)_4$ and cationic chitosan. In fact, the micelles were treated five times with the acid-based cycle, and both the fluorescence intensity and diameter were highly reversible under the acid-based-controlled condition.

4. Conclusions

In summary, nature cationic chitosan polyelectrolyte and TPE-$(N\text{-}COOH)_4$ with an AIE characteristic were used to construct fascinating micelles, exhibiting pH reversible transition between PIC and HBC aggregates. The highlight of this structure is the use of chitosan homopolymer not only as stabilized hydrophilic coronas but also as one indispensable building block of the aggregate cores. Additionally, under mildly basic condition (such as pH = 8), the positively charge chitosan can electrostatic interact with deprotonated TPE-$(N\text{-}COOH)_4$ to form PIC micelles, whereas the micelles were transformed to HBC with fully inverted micellar structures containing hydrogen upon pH decrease from 8 to 2. The diameter and fluorescence emission of the PIC micelles can be manipulated by changing the $[NH_3^+]/[COO^-]$ molar ratio. Moreover, the fluorescence emission of PIC micelles weakened as temperature rises, reflecting their temperature responsiveness. It is noteworthy that pH-driven formation of HBC with flipped micellar structures compressed the particle sizes and further intensified the fluorescence emission of TPE-$(N\text{-}COOH)_4$ moieties thanks to the elimination of electrostatic repulsion of carboxyl groups within the micelles. Furthermore, the pH-actuated fascinating transformation between PIC and HBC micelles with AIE enhancement feature was completely reversible under the control of acid-based cycle. The surface of the micelles was chemically active and provided the functional sites with chemical groups for subsequent chemical reactions (e.g., binding of biomolecules). Accordingly, this robust architecture of micelle may be expected to hold great potential for many different applications in a variety of fields including, for example, colloids, pH sensors, biomarkers, and antimicrobial materials.

Data Availability

The data used to support the findings of this study are available from the corresponding author upon request.

Conflicts of Interest

The authors declare that they have no conflicts of interest.

Acknowledgments

This work was financially supported by the Fundamental Research Funds from Jiangsu Province Biomass and Materials Laboratory (JSBEM202016 and JSBEM-S-202001), the Foundation of Anhui Laboratory of Clean Catalytic Engineering (LCCE-04), the Key Projects of Outstanding Young Talents Support Program of Anhui Province (gxyqZD2018051), and the Youth Talent Support Program of AHPU (2018-6).

References

[1] A. Abdollahi, H. Roghani-Mamaqani, and B. Razavi, "Stimuli-chromism of photoswitches in smart polymers: recent advances and applications as chemosensors," *Progress in Polymer Science*, vol. 98, article 101149, pp. 1–62, 2019.

[2] D. Zhong, H. Wu, Y. Wu et al., "Rational design and facile fabrication of biocompatible triple responsive dendrimeric nanocages for targeted drug delivery," *Nanoscale*, vol. 11, no. 32, pp. 15091–15103, 2019.

[3] Y. Lin, C. Li, A. Liu et al., "Responsive hyaluronic acid-gold cluster hybrid nanogel theranostic systems," *Biomaterials Science*, vol. 9, no. 4, pp. 1363–1373, 2021.

[4] Y. Zhao, F. Sakai, L. Su et al., "Progressive macromolecular self-assembly: from biomimetic chemistry to bio-inspired materials," *Advanced Materials*, vol. 25, no. 37, pp. 5215–5256, 2013.

[5] Y. Li, J. Lin, P. Wang et al., "Tumor microenvironment responsive shape-reversal self-targeting virus-inspired nanodrug for imaging-guided near-infrared-II photothermal chemotherapy," *ACS Nano*, vol. 13, no. 11, pp. 12912–12928, 2019.

[6] G. Yu, K. Jie, and F. Huang, "Supramolecular amphiphiles based on host-guest molecular recognition motifs," *Chemical Reviews*, vol. 115, no. 15, pp. 7240–7303, 2015.

[7] X. Ma and Y. Zhao, "Biomedical applications of supramolecular systems based on host-guest interactions," *Chemical Reviews*, vol. 115, no. 15, pp. 7794–7839, 2015.

[8] S. Wang, W. Gao, X.-Y. Hu, Y.-Z. Shen, and L. Wang, "Supramolecular strategy for smart windows," *Chemical Communications*, vol. 55, no. 29, pp. 4137–4149, 2019.

[9] R. Guo, L. Zhang, Z. Zhu, and X. Jiang, "Direct facile approach to the fabrication of chitosan-gold hybrid nanospheres," *Langmuir*, vol. 24, no. 7, pp. 3459–3464, 2008.

[10] K. Li, Z. Zhu, P. Cai et al., "Organic dots with aggregation-induced emission (AIE dots) characteristics for dual-color cell tracing," *Chemistry of Materials*, vol. 25, no. 21, pp. 4181–4187, 2013.

[11] D. Ding, Z. Zhu, R. Li et al., "Nanospheres-incorporated implantable hydrogel as a trans-tissue drug delivery system," *ACS Nano*, vol. 5, no. 4, pp. 2520–2534, 2011.

[12] L. S. Shlyakhtenko, A. Y. Lushnikov, A. Miyagi, and Y. L. Lyubchenko, "Specificity of binding of single-stranded DNA-binding protein to its target," *Biochemistry*, vol. 51, no. 7, pp. 1500–1509, 2012.

[13] Y. Chen, H. Qian, X. Zheng, X. Jiang, H. Yu, and L. Zhang, "Nonspherical polysaccharide vesicles and their shape and volume regulation via osmotically sensitive channels," *Soft Matter*, vol. 7, no. 12, pp. 5519–5523, 2011.

[14] A. Harada and K. Kataoka, "Formation of polyion complex micelles in an aqueous milieu from a pair of oppositely-charged block copolymers with poly(ethylene glycol) segments," *Macromolecules*, vol. 28, no. 15, pp. 5294–5299, 1995.

[15] Y. Anraku, A. Kishimura, M. Kamiya et al., "Systemically injectable enzyme-loaded polyion complex vesicles as in vivo nanoreactors functioning in tumors," *Angewandte Chemie International Edition*, vol. 128, no. 2, pp. 570–575, 2016.

[16] F. Pu, J. Ren, and X. Qu, "Nucleobases, nucleosides, and nucleotides: versatile biomolecules for generating functional nanomaterials," *Chemical Society Reviews*, vol. 47, no. 4, pp. 1285–1306, 2018.

[17] J. Nicolas, S. Mura, D. Brambilla, N. Mackiewicz, and P. Couvreur, "Design, functionalization strategies and biomedical applications of targeted biodegradable/biocompatible polymer-based nanocarriers for drug delivery," *Chemical Society Reviews*, vol. 42, no. 3, pp. 1147–1235, 2013.

[18] H. Chen, Z. Gu, H. An et al., "Precise nanomedicine for intelligent therapy of cancer," *Science China Chemistry*, vol. 61, no. 12, pp. 1503–1552, 2018.

[19] K. Wang, K. Amin, Z. An et al., "Advanced functional polymer materials," *Materials Chemistry Frontiers*, vol. 4, no. 7, pp. 1803–1915, 2020.

[20] S. Tian, G. Liu, X. Wang et al., "pH-regulated reversible transition between polyion complexes (PIC) and hydrogen-bonding complexes (HBC) with tunable aggregation-induced emission," *ACS Applied Materials & Interfaces*, vol. 8, no. 6, pp. 3693–3702, 2016.

[21] X. Liu, Y. Zeng, J. Liu et al., "Highly emissive nanoparticles based on AIE-active molecule and PAMAM dendritic "molecular glue"," *Langmuir*, vol. 31, no. 15, pp. 4386–4393, 2015.

[22] C. Li, T. Wu, C. Hong, G. Zhang, and S. Liu, "A general strategy to construct fluorogenic probes from charge-generation polymers (CGPs) and AIE-active fluorogens through triggered complexation," *Angewandte Chemie International Edition*, vol. 51, no. 2, pp. 455–459, 2012.

[23] J. Wang, J. Yu, Y. Zhang et al., "Charge-switchable polymeric complex for glucose-responsive insulin delivery in mice and pigs," *Science Advances*, vol. 5, no. 7, article eaaw4357, pp. 1–10, 2019.

[24] J. Wang, J. Wang, P. Ding et al., "A supramolecular crosslinker gives salt resistant PIC micelles and improved MRI contrast agents," *Angewandte Chemie International Edition*, vol. 57, no. 39, pp. 12680–12684, 2018.

[25] W. Zhou, J. Wang, P. Ding, X. Guo, M. A. Cohen Stuart, and J. Wang, "Functional polyion complex vesicles enabled by supramolecular reversible coordination polyelectrolytes," *Angewandte Chemie International Edition*, vol. 58, no. 25, pp. 8494–8498, 2019.

[26] Y. Hu, Y. Chen, Q. Chen, L. Zhang, X. Jiang, and C. Yang, "Synthesis and stimuli-responsive properties of chitosan/poly(acrylic acid) hollow nanospheres," *Polymer*, vol. 46, no. 26, pp. 12703–12710, 2005.

[27] Y. Lin, S. Wang, Y. Zhang et al., "Ultra-high relaxivity iron oxide nanoparticles confined in polymer nanospheres for tumor MR imaging," *Journal of Materials Chemistry B*, vol. 3, no. 28, pp. 5702–5710, 2015.

[28] L. M. B. Ferreira, A. M. dos Santos, F. I. Boni et al., "Design of chitosan-based particle systems: a review of the physicochemical foundations for tailored properties," *Carbohydrate Polymers*, vol. 250, article 116968, pp. 1–20, 2020.

[29] W. Jiang, W. Wang, B. Pan, Q. Zhang, W. Zhang, and L. Lv, "Facile fabrication of magnetic chitosan beads of fast kinetics and high capacity for copper removal," *ACS Applied Materials & Interfaces*, vol. 6, no. 5, pp. 3421–3426, 2014.

[30] D.-T. Vo, C. G. Whiteley, and C.-K. Lee, "Hydrophobically modified chitosan-grafted magnetic nanoparticles for bacteria removal," *Industrial & Engineering Chemistry Research*, vol. 54, no. 38, pp. 9270–9277, 2015.

[31] J. Mei, N. L. C. Leung, R. T. K. Kwok, J. W. Y. Lam, and B. Z. Tang, "Aggregation-induced emission: together we shine, united we soar!," *Chemical Reviews*, vol. 115, no. 21, pp. 11718–11940, 2015.

[32] L. He, L. Li, X. Liu, J. Wang, H. Huang, and W. Bu, "Acid-base-controlled and dibenzylammonium-assisted aggregation induced emission enhancement of poly(tetraphenylethene) with an impressive blue shift," *Polymer Chemistry*, vol. 7, no. 22, pp. 3722–3730, 2016.

[33] J. Zhou, G. Yu, and F. Huang, "AIE opens new application in super-resolution imaging," *Journal of Materials Chemistry B*, vol. 4, no. 48, pp. 7761–7765, 2016.

[34] R. Zhang, Y. Duan, and B. Liu, "Recent advances of AIE dots in NIR imaging and phototherapy," *Nanoscale*, vol. 11, no. 41, pp. 19241–19250, 2019.

[35] D. D. La, S. V. Bhosale, L. A. Jones, and S. V. Bhosale, "Tetraphenylethylene-based AIE-active probes for sensing

applications," *ACS Applied Materials & Interfaces*, vol. 10, no. 15, pp. 12189–12216, 2018.

[36] P. Zhang, K. Wu, J. Guo, and C. Wang, "From hyperbranched polymer to nanoscale CMP (NCMP): improved microscopic porosity, enhanced light harvesting, and enabled solution processing into white-emitting Dye@NCMP films," *ACS Macro Letters*, vol. 3, no. 11, pp. 1139–1144, 2014.

[37] S. Xu, X. Bai, J. Ma et al., "Ultrasmall organic nanoparticles with aggregation induced emission and enhanced quantum yield for fluorescence cell imaging," *Analytical Chemistry*, vol. 88, no. 15, pp. 7853–7857, 2016.

[38] D. Wang and B. Z. Tang, "Aggregation-induced emission luminogens for activity-based sensing," *Accounts of Chemical Research*, vol. 52, no. 9, pp. 2559–2570, 2019.

[39] Y. Hu, X. Jiang, Y. Ding, H. Ge, Y. Yuan, and C. Yang, "Synthesis and characterization of chitosan-poly(acrylic acid) nanoparticles," *Biomaterials*, vol. 23, no. 15, pp. 3193–3201, 2002.

[40] I. Richard, M. Thibault, G. de Crescenzo, M. Buschmann, and M. Lavertu, "Ionization behavior of chitosan and chitosan-DNA polyplexes indicate that chitosan has a similar capability to induce a proton-sponge effect as PEI," *Biomacromolecules*, vol. 14, no. 6, pp. 1732–1740, 2013.

[41] H.-T. Feng, J. B. Xiong, Y. S. Zheng et al., "Multicolor emissions by the synergism of intra/intermolecular slipped π–π stackings of tetraphenylethylene-DiBODIPY conjugate," *Chemistry of Materials*, vol. 27, no. 22, pp. 7812–7819, 2015.